Extended wavelength emission to 1.3 μm in nitrided InAs/GaAs self-assembled quantum dots

Kita, Takashi ; Mori, T. ; Seki, H. ; Matsushita, M. ; Kikuno, M. ; Wada, Osamu ; Ebe, H. ; Sugawara, M. ; Arakawa, Y. ; Nakata, Y.

(Citation)
Journal of Applied Physics,97(2):24306-24306

(Issue Date)
2005-01

(Resource Type)
journal article

(Version)
Version of Record

Extended wavelength emission to 1.3 μm in nitrided InAs/GaAs self-assembled quantum dots

T. Kita,[a] T. Mori, H. Seki, M. Matsushita, M. Kikuno, and O. Wada
Department of Electrical and Electronics Engineering, Faculty of Engineering, Kobe University, 1-1 Rokkodai, Nada, Kobe 657-8501, Japan

H. Ebe, M. Sugawara, and Y. Arakawa
Research Center for Advanced Science and Technology, University of Tokyo, 4-6-1 Komaba, Meguro-ku, Tokyo 153-8505, Japan

Y. Nakata
Fujitsu Laboratories Ltd., 10-1 Morinosato-Wakamiya, Atsugi 243-0197, Japan

(Received 16 July 2004; accepted 20 October 2004; published online 27 December 2004)

We have studied long-wavelength emission in 1.3-μm optical communication range from nitrided InAs/GaAs quantum dots (QDs). Atomic-layer nitridation just after the growth of InAs QDs realizes a remarkable redshift of the photoluminescence peak by more than 150 nm. Growth temperature plays a key role in achieving room-temperature emission from the QDs. The emission wavelength can be adjusted by controlling the growth conditions of the initial InAs QDs. As compared with conventional QDs grown without nitridizing the QD surface, it is found that the nitridation results in larger dots with a large aspect ratio. © *2005 American Institute of Physics*.
[DOI: 10.1063/1.1833578]

I. INTRODUCTION

In a bulk three-dimensional semiconductor, transitions due to stimulated recombination of electron-hole pairs results in light emission over a broad spread in wavelength. However, preparation of low-dimensional heterostructures enables charge carriers to be localized by the confinement. In particular, carriers localized in a zero-dimensional quantum dot (QD) exhibit atomlike density of states concentrated into fully quantized, discrete, and hence more widely separated energy levels. This realizes QD lasers with smaller threshold current density, less temperature dependence, and narrower linewidth together with higher differential efficiency and power output.[1–3] In particular, InAs QDs grown on GaAs substrate is expected to replace more costly InP-based lasers.[4] However, a large InAs–GaAs lattice mismatch (7%) induces an unwanted QD band-gap increase and wavelength decrease. The key issue of InAs/GaAs QDs is therefore the extension of the emission wavelength into 1.3 μm and even to 1.55 μm optical communication windows.

Several kinds of approaches have been proposed: (1) stacking,[5–7] (2) alternating deposition,[8] and (3) strain control by a capping layer.[9–12] In particular, the strain engineering by the capping layer has great advantages of achieving wavelength extension into the fiber-optic communications wavelengths. For example, when we overgrow pseudomorphic InGaAs onto InAs/GaAs QDs, increasing In content in the capping layer increases strain relief. Then, the emission wavelength extends toward 1.5 μm.[9,10] On the other hand, when the QDs are capped by GaNAs instead of GaAs, the total strain energy is expected to be reduced, and thereby, the wavelength is extended.[11,12] It is noted that, in both cases, the lower barrier heights of the capping layer enhance the wavelength extension.

In contrast to such strain engineering, nitrogen doping into InGaAs QDs has attracted much interest for a long-wavelength laser material to be grown on GaAs. The incorporation of small amounts of nitrogen leads to a remarkable band-gap reduction[13] because of the huge-band-gap bowing parameters of 18 eV for GaAsN (Ref. 14) and 4.2 eV for InAsN (Refs. 15 and 16). Sopanen *et al.* (Ref. 17) has grown InGaAsN QDs on GaAs(001) and demonstrated 1.5 μm emission at room temperature. However, the emission intensity at room temperature shows a significant reduction, and much stronger emission is expected for real laser-device applications.

Recently, we proposed a QD growth technique using nitridation.[18] In this process, we first grow conventional InAs/GaAs QDs by the Stranski–Krastanov process. After that, we nitridize the surface. Then, the nitrided QDs are capped by GaAs. This simple process realizes a remarkable redshift over more than 100 nm and a narrower spectral linewidth compared with that of InAs QDs.[18,19] However, broad distributed states appeared below the QD photoluminescence (PL) and resulted in an extremely weak QD PL near room temperature.[18] In this experiment, we have succeeded in eliminating the broad signal, and achieving 1.3-μm emission at room temperature by controlling the growth conditions of the initial InAs QDs. Detailed temperature dependences of PL from the nitrided QDs are analyzed and a key mechanism of the wavelength extension is discussed.

II. GROWTH AND CHARACTERIZATION

Self-assembled InAs QDs were grown on GaAs(001) substrates by a solid-source molecular beam epitaxy (MBE)

[a]Electronic mail: kita@eedept.kobe-u.ac.jp

TABLE I. Sample list.

Sample	InAs growth conditions		
	Deposition thickness (ML)	Deposition rate (ML/s)	Growth temperature (°C)
QD1	2.5	0.012	460
QD2	2.5	0.0048	460
QD3	2.5	0.0013	440
QD4	1.8	0.012	470
QD5	2.5	0.012	490
NQD1	2.5	0.012	460
NQD2	2.5	0.0048	460
NQD3	2.5	0.0013	460
NQD4	1.8	0.012	470
NQD5	2.5	0.012	490

equipped with a radio-frequency (rf) plasma source. Active nitrogen species were created in the plasma source from ultrapure N_2 gas. The nitrogen partial pressure was 5×10^{-5} Torr, and the gas-flow rate was 1 ccm. The rf power was set at 230 W. A 510-nm buffer layer of GaAs was grown at 530 °C. Detailed growth conditions for InAs are summarized in Table I. The InAs deposition thickness was estimated from the reflection high-energy electron diffraction (RHEED) oscillations during a homoepitaxial growth. To obtain QDs with different sizes, we controlled the InAs deposition rate. The slow growth rate enables us to grow larger-size QDs showing longer-wavelength emission. The transition from a two-dimensional (2D) wetting layer growth to a three-dimensional (3D) island growth is determined from the change in the RHEED pattern. At the growth transition, the RHEED exhibits chevron patterns representing the QD formation. After growing the InAs QDs, we performed nitridation of the QDs for 8 s at the same substrate temperature as that during the QD growth. That roughly corresponds to one monolayer coverage of the surface.[18] After that, the dots were capped by a 80-nm-thick GaAs. The As flux was kept constant at 3.0×10^{-6} Torr during the growth process.

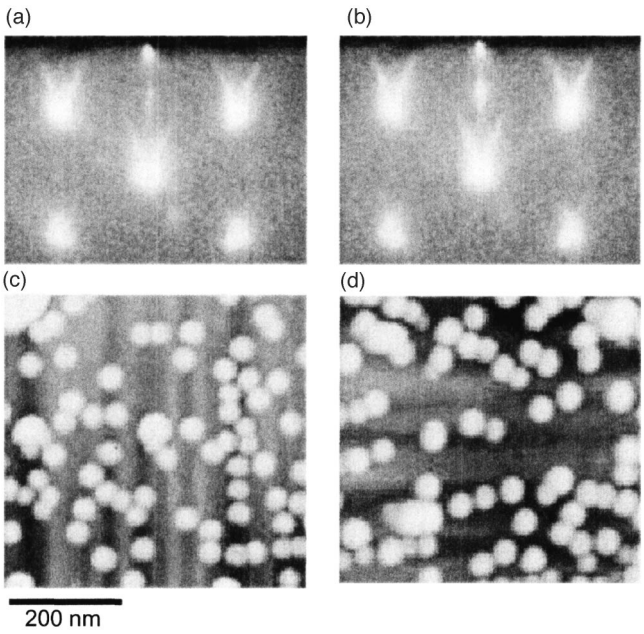

FIG. 1. RHEED-diffraction patterns [(a) and (b)], and AFM images [(c) and (d)] of InAs QDs surfaces before [(a) and (c)] and after [(b) and (d)] nitridation.

TABLE II. Average density, size, and height of QD before and after nitridation.

	Before nitridation	After nitrization
Density (cm^{-2})	2.4×10^{10}	2.3×10^{10}
Diameter (nm)	44	45
Height (nm)	7	6

PL measurements have been performed to characterize the QD samples. The sample was excited by the 488-nm line of an Ar-ion laser. The PL signal dispersed by a 320-mm single monochromator was detected by a liquid-nitrogen-cooled InGaAs-diode array.

III. RESULTS AND DISCUSSIONS

The RHEED patterns in the [−110] azimuth before and after nitridation of the InAs QDs are shown in Figs. 1(a) and 1(b), respectively. The growth temperature of this sample is 460 °C. During nitridation, the RHEED patterns keep the chevron patterns. This result indicates that nitridation does not give rise to significant crystallographical damage to the QDs. That is independent of the growth temperature. After growing the 80-nm capping layer, the surface becomes flat.

Atomic force microscope (AFM) images of the QD surface before and after nitridation are shown in Figs. 1(c) and 1(d), respectively. The QD density and the average size are almost the same, and are independent of the nitridation process. Quantitative results are summarized in Table II.

A. Growth temperature dependence of PL

PL spectra of InAs QDs and nitrided InAs QDs grown at different temperatures are shown in Fig. 2. The PL measurements were carried out at 4 K. The dashed and solid lines indicate PL spectra of the InAs QDs and the nitrided QDs, respectively. The nitridation-induced redshift is over 150 nm.

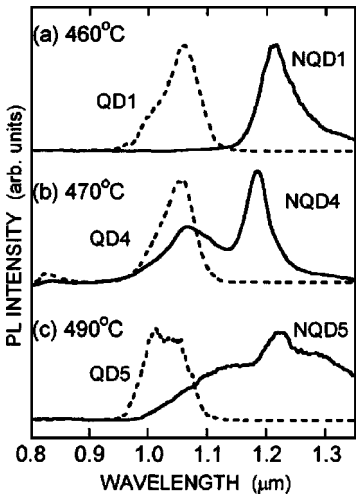

FIG. 2. 4 K PL spectra of InAs QDs (QD1, QD4, and QD5) and nitrided InAs QDs (NQD1, NQD4, and NQD5).

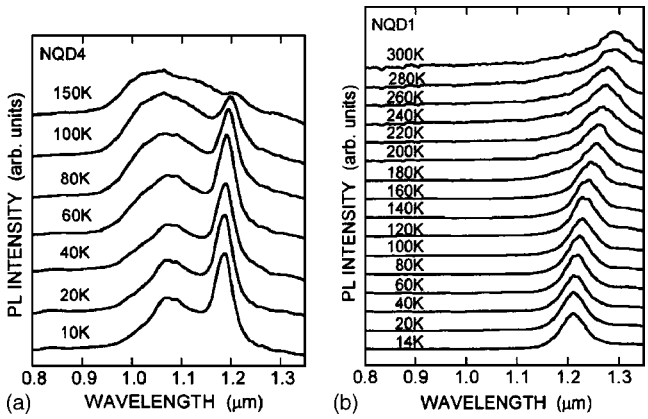

FIG. 3. Temperature dependence of PL spectra for nitrided InAs QDs grown at 470 °C (NQD4) (a) and 460 °C (NQD1) (b).

With increasing the growth temperature, a broad signal below the QD PL becomes strong. In particular, the PL of the nitrided QDs grown at 490 °C (NQD5) is dominated by the broad signal. The broad signal comes from the nitrided wetting layer,[18] and leads to an unexpected temperature dependence elaborated in the following discussion. On the other hand, a single PL peak has been obtained for the nitrided QDs grown at 460 °C (NQD1). Figures 3(a) and 3(b) show the PL temperature dependence for the nitrided QDs grown at 470 °C (NQD4) and 460 °C (NQD1), respectively. With increasing the sample temperature, the QD PL of the 470 °C-grown sample shows a rapid decrease of the emission intensity. The simultaneous increase of the broad signal intensity reflects thermal carrier population of photoexcited carriers from the QD states into unwanted states in the wetting layer. On the other hand, the single PL peak of the 460 °C-grown sample shows a temperature dependence obeying the Varshni relation.[20] Furthermore, the PL at room temperature is observed at 1.3 μm.

A typical temperature dependence of the PL intensity is shown in Fig. 4. The open and closed circles indicate PL intensities for InAs QDs (QD3) and nitrided QDs (NQD3), respectively. For the InAs QDs at room temperature, the PL intensity decreases by 1% of that at low temperature. This has been observed commonly in all InAs QDs examined. The nitrided QDs also show a similar temperature dependence.

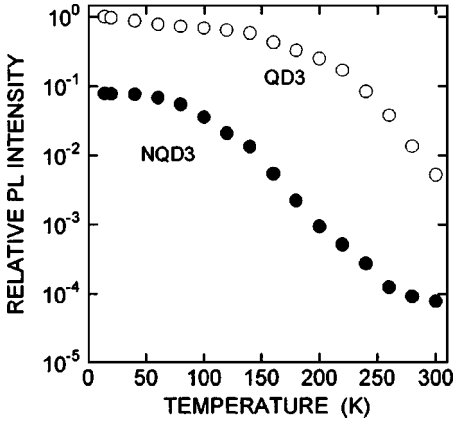

FIG. 4. Temperature dependence of PL intensity for InAs QDs (QD3) (open circles) and nitrided InAs QDs (NQD3) (closed circles).

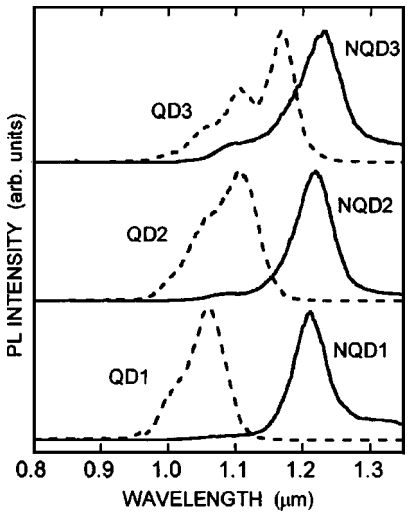

FIG. 5. PL spectra of nitrided InAs QDs (NQD1, NQD2, and NQD3) for different size InAs QDs (QD1, QD2, and QD3) grown at different InAs-deposition rates.

The room-temperature PL intensity of the nitrided QDs maintains about 5% of that of the InAs QDs.

B. Control of emission wavelength

PL spectra of nitrided QDs for InAs QDs with different sizes are shown in Fig. 5. PL measurements were carried out at 14 K. The QD size has been controlled by the InAs-deposition rate as listed in Table I. Larger QDs can be grown by a slower deposition rate. The PL peak of the InAs QDs shifts toward the longer wavelength side with decreasing the deposition rate. It is found that the nitridation-induced PL redshift depends on the *initial* InAs QDs, in other words, we can control the emission wavelength of the nitrided QDs by adjusting the growth conditions of the InAs QDs. The nitridation-induced redshift becomes small with increasing the initial QD size, and, thereby, the PL wavelength of the nitrided QDs seems to converge to a wavelength near 1.25 μm at 14 K (1.35 μm at room temperature).

Figure 6 summarizes the temperature dependence of the PL-peak wavelength. The closed and open symbols indicate PL-peak wavelengths for the InAs QDs and the nitrided QDs, respectively. The circles and squares indicate data for samples grown at 0.012 and 0.0013 ML/s, respectively. The solid lines indicate fitted curves calculated by the Varshni relation. In all temperatures, the redshift is almost the same. Therefore, the temperature coefficient of the band gap is almost independent of the nitridation. On the other hand, if we assume that the deposited nitrogen atoms are completely doped into InAs QDs, the doped nitrogen concentration in InAsN QDs is roughly estimated to be 0.7%. Since a nitrogen containing material has a smaller temperature coefficient,[21] the observed temperature coefficient excludes the possibility of the InAsN-alloy dots formation.

C. What happens in the nitrided QDs?

A significant difference in morphology of growth surface has been observed at the initial stage of the capping layer growth. Generally, as the capping layer growth proceeds, the

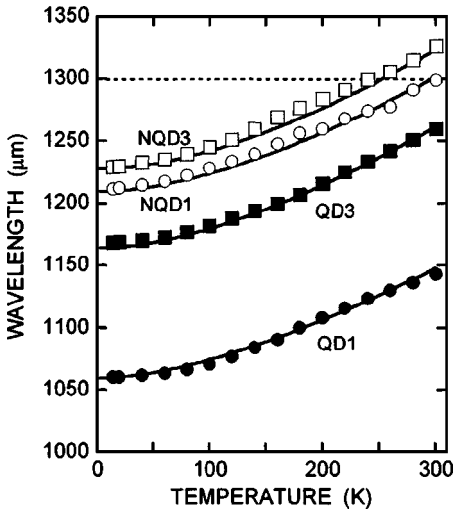

FIG. 6. Temperature dependence of the PL-peak wavelength. The closed and open symbols indicate PL-peak wavelength for the InAs QDs and the nitrided QDs, respectively. The circles and squares indicate the data for samples grown at 0.012 and 0.0013 ML/s, respectively.

surface becomes flat, and the RHEED pattern returns to the streak image. Nevertheless, in the case of the nitrided QD, the RHEED-diffraction spot intensity becomes strong for a while after the capping layer growth. AFM images taken after the growth of a 10-nm-thick GaAs are shown in Figs. 7(a) and 7(b) for the InAs QDs and the nitrided QDs, respectively. The samples were grown at 460 °C. The surface of the conventional InAs QDs covered by the thin capping layer becomes flat. In contrast to that, it is clearly confirmed that the surface of the nitrided QDs becomes rough. In both cases, when growing the 80-nm-thick capping layer, the surface becomes finally flat. The 10-nm-thick capping layer is comparable to the average QD height. It is well known that In segregation during the capping layer growth truncates the pyramidal-shape islands. Therefore, the flat surface of Fig. 7(a) for the InAs QDs is understood by truncation of the

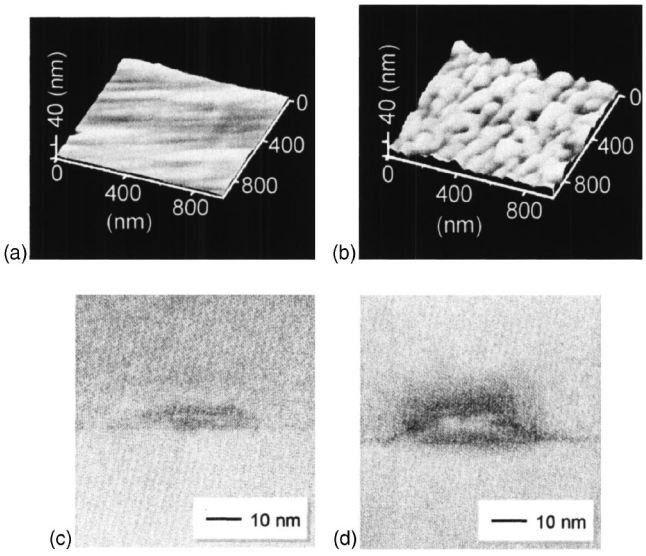

FIG. 7. AFM images for InAs QDs (a) and nitrided InAs QDs (b) capped by a 10-nm-thick GaAs capping layer. Cross-sectional TEM images for QD1 (c) and NQD1 (d).

InAs islands. The rough surface observed for the nitrided QDs suggests that the deposited nitrogen restrains the segregation, and the QDs remain untruncated. Since the motive force of the segregation is the large lattice mismatch between InAs and GaAs, small nitrogen atoms deposited on the InAs QD surface, which may be considered to be a InAsN thin layer, relax the interface strain and restrain the segregation effects. That results in larger QDs. To confirm the size and shape of the nitrided QDs, we performed cross-sectional transmission electron microscope (TEM) observation. Figures 7(c) and 7(d) shows typical results for the InAs QDs (QD1) and the nitrided QDs (NQD1), respectively. A significant increase of the QD height is observed. It is noted that the cross-section size of the nitrided QD is almost the same as the bare InAs dots listed in Table II. Based on these investigations, the PL redshift is considered to be caused by the larger QDs. However, if this is the only mechanism, it is difficult to understand that the PL wavelength of the nitrided QDs seems to converge to a wavelength close to 1.35 μm. As I mentioned in the previous paper (Ref. 18), strain relaxation caused by the InAsN thin layer which covers the QD should be considered. Since the surface/volume ratio of the QD is larger for smaller size QD, the internal compressive strain in smaller QD is reduced by the InAsN thin layer in a more pronounced way. Therefore, one can consider that PL signal from the smaller size QD shifts significantly toward the longer wavelength side. Such effect would be considered as well as the reduction of QD size modification. Detailed experiments to make the mechanism clear are on going.

V. SUMMARY

We have studied long-wavelength emission in 1.3-μm optical communication range from nitrided InAs/GaAs QDs. Atomic-layer nitridation on the InAs QD surface extends the wavelength by more than 150 nm. Growth temperature is a key factor to minimize unwanted broadened signal. Bright emission has been observed at 1.3 μm at room temperature when we grow it at 460 °C. The PL redshift depends on the sizes of the initial InAs QDs, and the PL wavelength of the nitrided QDs seems to converge to a wavelength near 1.35 μm at room temperature. A significant morphological difference has been observed at the initial stage of the capping layer growth. According to AFM and TEM observations, it has been indicated that nitridation on the InAs QDs restrains the In segregation effects and results in large dots comparable to the bare InAs dots. The PL redshift is considered to be caused by the larger QDs as well as strain relaxation caused by the InAsN thin layer.

ACKNOWLEDGMENTS

This work was supported by the Venture Business Laboratory Project at Kobe University and in part by the Scientific Research Grant-in-Aid Nos. 15360166, 15656018, and 16360155 from the Ministry of Education, Culture, Sports, Science and Technology of Japan and Nippon Sheet Glass Foundation for Materials Science and Engineering.

[1]Y. Arakawa and H. Sakaki, Appl. Phys. Lett. **40**, 939 (1982).

[2]D. Bimberg, M. Grundmann, and N. N. Ledentsov, *Quantum Dot Heterostructures* (Wiley, New York, 1998).
[3]M. Sugawara, *Semiconductor and Semimetals*, edited by M. Sugawara (Academic, San Diego, 1999), Vol. 60.
[4]N. N. Ledentsov *et al.*, Electron. Lett. **39**, 1126 (2003).
[5]Y. Nakata, Y. Sugiyama, K. Mukai, T. Futatsugi, H. Shoji, M. Sugawara, H. Ishikawa, and N. Yokoyama, Inst. Phys. Conf. Ser. No. 162 (1999) (unpublished), Chap. 9, p. 427.
[6]Y. Nakata, K. Mukai, M. Sugawara, K. Ohtsubo, H. Ishikawa, and N. Yokoyama, J. Cryst. Growth **208**, 93 (2000).
[7]T. Kita, O. Wada, H. Ebe, Y. Nakata, and M. Sugawara, Jpn. J. Appl. Phys., Part 2 **41**, L1143 (2002).
[8]S. Fafard, M. Spanner, J. P. McCaffrey, and Z. R. Wasilewski, Appl. Phys. Lett. **76**, 2268 (2000).
[9]J. Tatebayashi, M. Nishioka, and Y. Arakawa, Appl. Phys. Lett. **78**, 3469 (2001).
[10]J. Tatebayashi, M. Nishioka, and Y. Arakawa, J. Cryst. Growth **237–239**, 1296 (2002).
[11]X. Q. Zhang, S. Ganapathy, H. Kumano, K. Uesugi, and I. Suemune, J. Appl. Phys. **92**, 6813 (2002).
[12]S. Ganapathy, X. Q. Zhang, K. Uesugi, H. Kumano, I. Suemune, B. J. Kim, and T. Y. Seong, Proceedings of the 14th International Conference on InP and Related Materials (2002) (unpublished), p. 557–560.
[13]M. Kondow, K. Uomi, A. Niwa, T. Kitatani, S. Watahiki, and Y. Yazawa, Jpn. J. Appl. Phys., Part 1 **35**, 1273 (1996).
[14]M. Kondow, K. Uomi, K. Hosomi, and T. Mozume, Jpn. J. Appl. Phys., Part 2 **33**, L1056 (1994).
[15]T. Yang, S. Nakajima, and S. Sakai, Jpn. J. Appl. Phys., Part 2 **36**, L320 (1997).
[16]H. Naoi, Y. Naoi, and S. Sakai, Solid-State Electron. **41**, 319 (1997).
[17]M. Sopanen, H. X. Xin, and C. W. Tu, Appl. Phys. Lett. **76**, 994 (2000).
[18]T. Kita, Y. Masuda, T. Mori, and O. Wada, Appl. Phys. Lett. **83**, 4152 (2003).
[19]G. Sasikala, P. Thilakan, H. Kumano, K. Uesugi, I. Suemune, and Y. Nabetani, Thin Solid Films (in press).
[20]Y. P. Varshni, Physica (Utrecht) **34**, 149 (1967).
[21]K. Uesugi, I. Suemune, T. Hasegawa, T. Akutagawa, and T. Nakamura, Appl. Phys. Lett. **76**, 1285 (2000).